chap. 22; M. Newman *et al.*, *J. Atmos. Sci.* **41**, 1901 (1984).
2. V. P. Starr, *The Physics of Negative Viscosity Phenomena* (McGraw-Hill, New York, 1968); R. Hide, *J. Atmos. Sci.* **26**, 841 (1969).
3. P. J. Gierasch, *J. Atmos. Sci.* **32**, 1038 (1975); W. B. Rossow and G. P. Williams, *ibid.* **36**, 377 (1979).
4. S. S. Limaye, C. Grassotti, M. J. Kuetermeyer, *Icarus* **73**, 193 (1988); W. B. Rossow, A. D. Del Genio, T. P. Eicheler, *J. Atmos. Sci.* **47**, 2053 (1990).
5. S. B. Fels and R. S. Lindzen, *Geophys. Astrophy. Fluid Dyn.* **6**, 149 (1974); V. Ramanathan and R. D. Cess, *Icarus* **25**, 89 (1975).
6. C. B. Leovy, *Icarus* **69**, 193 (1987).
7. R. L. Walterscheid *et al.*, *J. Atmos. Sci.* **42**, 1982 (1985).
8. C. B. Leovy, *ibid.* **30**, 1218 (1973); P. J. Valdes, thesis, Oxford University (1985). Cyclostrophically balanced zonal winds correspond to a balance between the equatorward component of the centrifugal acceleration of the winds and the poleward component of the pressure gradient force per unit mass.
9. L. D. Travis *et al.*, *Science* **203**, 781 (1979).
10. J. R. Holton and W. Wehrbein, *Pure Appl. Geophys.* **118**, 284 (1980).
11. M. Tomasko, in *Venus*, D. M. Hunten *et al.*, Eds. (Univ. of Arizona Press, Tucson, AZ, 1983); D. Crisp, thesis, Princeton University, Princeton, NJ (1983).
12. N. L. Baker and C. B. Leovy, *Icarus* **69**, 202. We adapted the heating formulation of Baker and Leovy but modified it to prevent forcing of static instabilities.
13. Height values given here are the approximate equivalent to geometric height given as the negative of the log of the atmospheric pressure divided by the surface pressure.
14. M. Newman, thesis, University of Washington, Seattle, WA (1991). The model follows that of Baker and Leovy (*12*), with the exception of the features described above and: (i) the basic-state vertical profiles of temperature, specific heat, and the standard static stability, which were not mutually consistent in the Baker-Leovy model, have been corrected; (ii) the boundary condition at the pole was changed to allow nonzero values of angular velocity there.
15. C. C. Counselman *et al.*, *J. Geophys. Res.* **85**, 8026 (1980).
16. I. M. Held and A. Y. Hou, *J. Atmos. Sci.* **32**, 1038 (1980); A. Y. Hou, *ibid.* **41**, 3437 (1984).
17. A. Y. Hou *et al.*, *J. Atmos. Sci.* **47**, 1894 (1990).
18. J. T. Schofield and F. W. Taylor, *Q. J. R. Meteorol. Soc.* **109**, 57 (1983); J. B. Pechman and A. P. Ingersoll, *J. Atmos. Sci.* **41**, 3290 (1984); L. S. Elson, *ibid.* **40**, 1535 (1983).
19. S. B. Fels, *J. Atmos. Sci.* **43**, 2757 (1986).
20. A. D. Del Genio and W. B. Rossow, *ibid.* **47**, 293 (1990).
21. A. Hou and B. Farrell, *ibid.* **44**, 1049 (1987); G. Schubert and J. A. Whitehead, *Science* **163**, 71 (1969); C. Covey, R. L. Walterscheid, G. Schubert, *J. Atmos. Sci.* **43**, 3273 (1986).
22. This research was supported by the Planetary Atmospheres Program of the Solar System Exploration Division of the National Aeronautics and Space Administration. Simulations were carried out on the Cray Y-MP computer at the San Diego Supercomputer Facility of the National Science Foundation, whose provision of computer time is gratefully acknowledged.

3 March 1992; accepted 16 June 1992

Elasticity of α-Cristobalite: A Silicon Dioxide with a Negative Poisson's Ratio

Amir Yeganeh-Haeri, Donald J. Weidner, John B. Parise

Laser Brillouin spectroscopy was used to determine the adiabatic single-crystal elastic stiffness coefficients of silicon dioxide (SiO_2) in the α-cristobalite structure. This SiO_2 polymorph, unlike other silicas and silicates, exhibits a negative Poisson's ratio; α-cristobalite contracts laterally when compressed and expands laterally when stretched. Tensorial analysis of the elastic coefficients shows that Poisson's ratio reaches a maximum value of −0.5 in some directions, whereas averaged values for the single-phased aggregate yield a Poisson's ratio of −0.16.

The three distinct crystalline forms of SiO_2—quartz, tridymite, and cristobalite—occur widely in nature. Because of the broad technological applications and sheer abundance of quartz, its physical properties have been extensively studied; yet comparatively, there is little information available on the physical properties of cristobalite and tridymite. All three polymorphs of SiO_2 form complex three-dimensional, corner-linked networks of rigid SiO_4 tetrahedra. Furthermore, each of these crystalline forms has a high-temperature (β) and a low-temperature (α) modification (*1*, *2*).

We measured the single-crystal elastic properties of SiO_2 in the α-cristobalite structure under ambient conditions (*3*). We find that α-cristobalite exhibits a negative Poisson's ratio, contracting laterally when compressed and expanding laterally when stretched. Foams and two-dimensional honeycomb structures, that is, amorphous materials, and some elements such as As and Sb, also have negative Poisson's ratios (*4*, *5*), but other minerals apparently do not.

In an isotropic medium, Poisson's ratio (ν) is defined as the quotient of lateral contraction divided by longitudinal extension. Solids usually contract laterally when stretched and expand laterally when compressed, resulting in a positive Poisson's ratio. Poisson's ratio falls between 0.20 and 0.27 for most crystalline compounds and hard metals, has values between 0.30 and 0.40 for most soft metals, and is exactly 0.5 for liquids. Albeit it is counterintuitive that a solid should have a negative Poisson's ratio, according to the theory of elasticity the allowable range for Poisson's ratio in an isotropic medium is between +0.5 and −1.0 (*6*, *7*). These limits can be understood in terms of the relation between the bulk modulus (K) and the shear modulus (μ) of a solid, expressed as

$$\nu = (3K - 2\mu)/(6K + 2\mu) \quad (1)$$

If the solid is incompressible, that is, as K approaches infinity, it can be seen from Eq. 1 that ν approaches the upper limit of 0.5. In this type of solid, the bulk modulus is substantially larger than the shear modulus. For example, in liquids the shear modulus is zero; hence Poisson's ratio is exactly 0.5. Conversely, as K approaches zero, in the case of an infinitely compressible solid, ν tends toward −1.0. In this type of solid, the shear modulus far exceeds the bulk modulus. Other extraordinary behavior is also predicted to occur in compounds with a negative Poisson's ratio. For instance, as the Poisson's ratio approaches the lower limit of −1.0, the material's fracture toughness and its resistance to indentation are greatly enhanced. In other words, despite being pliant, the material can become tough (*4*, *5*, and references therein). Materials exhibiting a negative Poisson's ratio also have a large potential for applications as shock absorbers and fasteners.

We determined the single-crystal elastic properties of α-cristobalite using Brillouin spectroscopy (*8*). The experiments were carried out on a natural single crystal from the Ellora Caves of Hyderabad, India. The specimen was 200 μm in maximum dimension, colorless, and transparent, and its shape was a perfect octahedron. A total of 58 compressional and shear acoustic velocities in 27 distinct crystallographic directions were used to constrain the velocity surface (Fig. 1). The velocity surface of α-cristobalite is such that one of the shear (S) modes travels at a faster velocity than the corresponding compressional (P) wave (*9*). This velocity surface was inverted to determine the six independent elastic stiffness coefficients that characterize tetragonal α-cristobalite, space group $P4_12_12$ (Table 1) (*10*).

The large magnitude of the six elastic compliance coefficients (*11*) strongly reflects the pliant nature of the α-cristobalite framework (Table 1; Fig. 2A). This framework is highly anisotropic. The c axis, with a linear compressibility of $\beta_c = 2.73$ MPa^{-1}, is much more compressible than the a axis for which $\beta_a = 1.77$ MPa^{-1}. The α-cristobalite structure is also more rigid than it is incompressible; the shear modulus is approximately 2.4 times the bulk modulus (Table 1). Because the Si–O forces are

Center for High Pressure Research and Department of Earth and Space Sciences, State University of New York at Stony Brook, Stony Brook, NY 11794.

generally very stiff, the large magnitude of the elastic compliance parameters overwhelmingly suggests that, of the many forces involved, only the weak forces such as distant anion-anion interactions and pliant bending forces govern the mechanical properties of α-cristobalite.

Structural studies performed on α-cristobalite at high pressure can be used as a guide to interpret which specific angles, bonds, or combinations of both give rise to the large compressibility and negative Poisson's ratio (*12*). The effect of pressure on the crystal structure of α-cristobalite is manifest in the contraction of intertetrahedral O...O distances and in the bending of pliant Si–O–Si linkages. Indeed, of all SiO_2 polymorphs characterized at high pressure, α-cristobalite exhibits the largest change in the Si–O–Si angle and interpolyhedral O...O distances upon compression, a result of its extremely open crystal structure. Over a 1.1-GPa pressure interval, both O...O pairs lying nearly along the *c* axis and Si–O–Si angles decrease substantially, while O...O pairs in the other direction show a slight increase over this same pressure range (Fig. 2A). The positive value of coefficient S_{13} is representative of such behavior (Table 1), indicating that, when compressed along the *c* axis, the structure contracts slightly along the *a* axis. The cooperative bending of the Si–O–Si linkages and contraction of intertetrahedral O distances results in rotation of the rigid SiO_4 tetrahedra and causes the structure to partially collapse and fold inward. These structural changes also contribute to the enhanced compression along the *c* axis.

In order to deduce the elastic properties of a random, macroscopically isotropic aggregate of crystals, it has been common practice to place upper and lower bounds on the elasticity of the aggregate by averaging either the single-crystal elastic compliance (S_{ij}) or stiffness (C_{ij}) coefficients over all lattice space. The averaged values of the aggregate are known as the Reuss and Voigt bounds, respectively (6). For example, the Voigt bounds of the isotropic aggregate elastic moduli are given by (*13,14*)

$$K_V = (C^*_{11} + 2C^*_{12})/3 \quad (2a)$$

$$\mu_V = (C^*_{11} - C^*_{12} + 3C^*_{44})/5 \quad (2b)$$

The Poisson's ratio of the aggregate, in terms of the bulk and shear moduli corresponding to each bound, can be calculated with Eq. 1. In most solids the magnitude of the averaged pure shear coefficients, C^*_{44}, approximately equals that of the averaged off-diagonal shear coefficients, C^*_{12}. In these solids the bulk modulus far exceeds the shear modulus; hence, most materials have positive Poisson's ratios. However, closer scrutiny of the elasticity relations of the aggregate (Eqs. 1 and 2) and the single-crystal elastic coefficients (Table 1) emphasizes the unusual nature of α-cristobalite. Its negative Poisson's ratio can be attributed to the small value of the pure compression coefficient, C^*_{11}, and to the extremely unequal magnitude of the pure shear mode, C^*_{44}, and the off-diagonal shear mode, C^*_{12}. As a consequence, the bulk modulus is much smaller than the shear modulus.

Unfortunately, the above characterization is merely an idealization; anisotropic elastic coefficients are known for many solids. Moreover, in a single crystal the magnitude of Poisson's ratio depends on the specific directions of the applied stress and

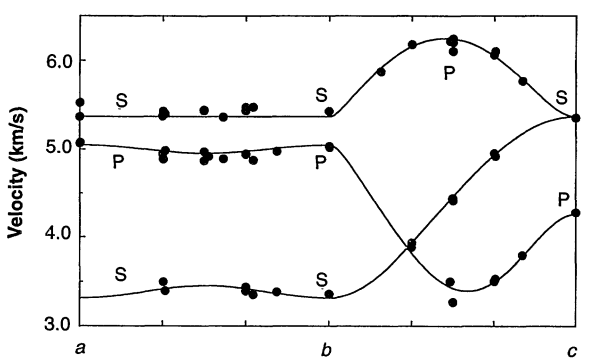

Fig. 1. Variation of acoustic velocity as a function of crystallographic direction in α-cristobalite. Velocities are projected onto the *a*–*b* and *b*–*c* planes. The solid line is the best fit model; circles represent experimentally measured velocities. Acoustic velocities for the best fit model deviate from the observed velocities by 0.046 km/s. P and S denote compressional and shear waves, respectively.

Table 1. Elastic and isotropic aggregate properties of α-cristobalite.

Elastic properties			Isotropic properties					
ij	*C*(GPa)	*S*(GPa^{-1})		*K* (GPa)	μ (GPa)	ν	V_P (km/s)	V_S (km/s)
11	59.4 (5)	0.0170	Reuss	15.95	34.99	−0.133	5.18	3.87
33	42.4 (7)	0.0240	Voigt	16.80	43.10	−0.191	5.64	4.30
44	67.2 (4)	0.0149	Hill	16.37	39.05	−0.163	5.41	4.09
66	25.7 (4)	0.0390						
12	3.8 (8)	−0.0010						
13	−4.4 (9)	0.0017						

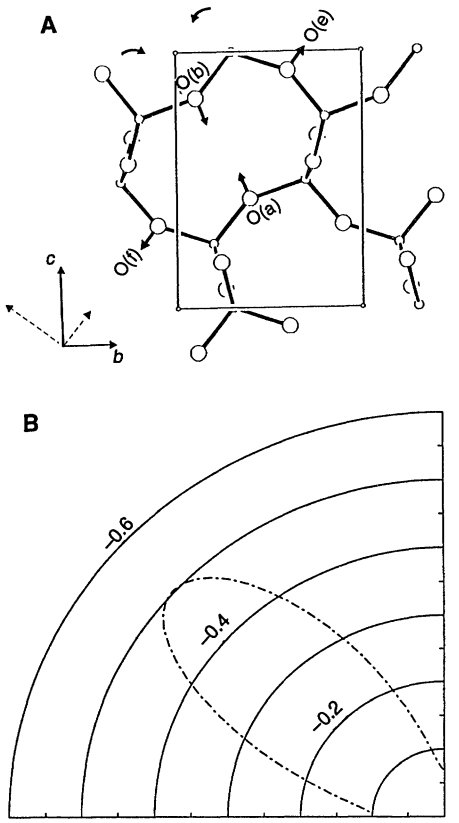

Fig. 2. Like other silicas, α-cristobalite is composed of individual SiO_4 units linked to four neighboring tetrahedra by the Si–O–Si linkage. The common O atom is known as the bridging O. This linkage pattern results in a three-dimensional framework of interconnected SiO_4 tetrahedra with each SiO_2 form having a distinct linkage pattern. For instance, when compared to α-quartz, α-cristobalite has a much more open structure. (**A**) Crystal structure of α-cristobalite projected down the *a* axis. The unit cell of α-cristobalite is shown as the rectangular outline. The Si and O atoms are distinguished as small and large circles, respectively. The arrows indicate the displacement of the O atoms and the rotations of SiO_4 tetrahedra as the structure is compressed. For example, O(a)...O(b) decreases by 6.5%, O(a)...O(c) decreases by 6.3%, and the Si–O–Si angle decreases by 4% over a pressure range of 1.1 GPa. However, over this same interval, O(e)...O(f) increases by 1.2%. The O(c) oxygen is located below the Si atom bounded by the O(b) and O(e) oxygens. (**B**) The variation in Poisson's ratio (ν_{23}, dashed-dot curve), showing a maximum of −0.5 as the elastic compliance tensor is rotated about the *a* axis. The crystallographic direction corresponding to this maximum is illustrated by the dashed axes in (A).

strain. In consideration of the marked elastic anisotropy of α-cristobalite, it seemed essential to evaluate the directional dependence of the Poisson's ratio.

In a Cartesian coordinate system the elastic strain (e_{ij}) and the stress ($\sigma_{k\ell}$) tensors are related by

$$e_{ij} = S_{ijk\ell}\sigma_{k\ell} \quad (3)$$

The coordinate system is usually chosen to coincide with the material's principal crystallographic axes. In terms of the single-crystal elastic compliance coefficients, the quotient of lateral to longitudinal strain, $-S_{iijj}/S_{iiii}$, is the exact definition of Poisson's ratio under all possible orientations of the coordinate system relative to the crystal's axes. To calculate Poisson's ratio for an arbitrarily chosen set of axes, we transformed the elements of the compliance tensor according to standard tensor transformation rules (*5*, *15*).

In α-cristobalite the directional dependence of Poisson's ratio exhibits marked anisotropy. Over all crystallographic directions its magnitude ranges from +0.08 to −0.5, although it remains predominantly negative. Comparatively, the Reuss and Voigt bounds of the single-phased aggregate yield Poisson's ratios of −0.13 and −0.19, respectively (Table 1). Rotation of the elastic compliance tensor about the *a* axis produces a maximum $\nu_{23} = -0.5$ at approximately 42° from the *b* axis (Fig. 2B). The occurrence of this maximum can be appreciated in light of the topology of the α-cristobalite structure. As the unit cell is rotated around the *a* axis, the compressive axes become aligned with the O pair displaying the largest contractions (Fig. 2A). Compression of these O...O separations along with concomitant bending of the Si–O–Si angle result in an inward rotation of the SiO_4 tetrahedra. Consequently, the structure contracts laterally.

It is suggested that for materials having a large degree of elastic anisotropy, such as α-cristobalite, α-quartz, stishovite (the high-pressure modification of SiO_2), and $MgSiO_3$ in the ilmenite structure, whenever single-crystal elastic coefficients are available, it is valuable to carry out a tensorial analysis of the elastic coefficients and examine the entire range of behavior of Poisson's ratio.

REFERENCES AND NOTES

1. L. G. Liu and W. Bassett, *Elements, Oxides, Silicates: High-Pressure Phases with Implications for the Earth's Interior* (Oxford Univ. Press, New York, 1986).
2. H. D. Megaw, *Crystal Structures. A Working Approach* (Saunders, Philadelphia, 1973).
3. β-Cristobalite is the high-temperature polymorph of SiO_2 above 1743 K. However, β-cristobalite exists metastably to about 540 K, where it undergoes a rapid and reversible inversion to low or α-cristobalite.
4. R. Lakes, *Science* **235**, 1038 (1987).
5. D. Gunton and G. Saunders, *J. Mater. Sci.* **7**, 1061 (1972).
6. A. H. Love, *A Treatise on the Mathematical Theory of Elasticity* (Dover, New York, 1944).
7. From a thermodynamic point of view, conservation of volume is not required.
8. For details on Brillouin spectroscopy see, for example, D. Weidner and H. Carleton, *J. Geophys. Res.* **82**, 1334 (1977); M. Vaughan and J. Bass, *Phys. Chem. Miner.* **10**, 62 (1982).
9. To confirm that one of the shear waves travels with a faster velocity than the corresponding compressional wave, the polarizations of the acoustic modes were independently verified by the polarization of the scattered light according to Brillouin scattering selection rules, and by the tetragonal symmetry of the material, which requires that two modes converge to a degenerate shear mode along the *c* axis. The velocity of this shear mode is the same as the shear mode in the *a*–*b* plane, which is polarized in the *c* direction (see Fig. 1).
10. J. Nye, *Physical Properties of Single Crystals* (Oxford Univ. Press, Oxford, 1977).
11. The elasticity of a single crystal is usually described in terms of the stiffness (C_{ij}) or the compliance (S_{ij}) coefficients (the inverse of C_{ij}). The elastic compliance coefficients portray the change in the crystal's shape as it is stressed. In a crystal with tetragonal symmetry, the coefficients S_{11} and S_{33} represent the response to uniaxial compression; their magnitudes are indicative of the compressibility of the crystal along the *a* and *c* axes, respectively. The shear compliance in the *a*–*c* and *a*–*b* crystallographic planes is governed by coefficients S_{44} and S_{66}. The off-diagonal coefficients S_{12} and S_{13}, on the other hand, describe the strain induced along the *b* and *c* axes, respectively, due to a stress parallel to the *a* axis; they monitor how much a material can contract or expand laterally when compressed. A positive sign associated with these coefficients would be indicative of lateral contraction, whereas a negative sign indicates lateral expansion.
12. A. Yeganeh-Haeri *et al.*, *Eos* **71** (no. 43) (Fall Meeting Suppl.), 1671 (1991); The high-pressure crystal chemistry of SiO_2 in the α-cristobalite structure was investigated through in situ x-ray diffraction using a DIA type apparatus. Unit cell parameters were determined at ambient and elevated pressures and were then used in the distance least squares procedure to model atomic coordinates (A. Yeganeh-Haeri *et al.*, in preparation).
13. A similar expression using S_{ij} values can be written for the Reuss bounds of the aggregate.
14. In a crystal with tetragonal symmetry, $C^*_{11} = (2C_{11} + C_{33})/3$; $C^*_{44} = (2C_{44} + C_{66})/3$; $C^*_{12} = (2C_{13} + C_{12})/3$.
15. P. J. Musgrave, *Crystal Acoustics* (Holden-Day, San Francisco, 1970).

16. We thank C. Francis for providing the single crystals of α-cristobalite (Harvard Mineralogical Museum sample 97849). Financial support for this research was provided by National Science Foundation grants EAR-8804087 (D.J.W.) and DMR-9024249 (J.B.P.). Mineral Physics Institute contribution 67.

2 April 1992; accepted 22 June 1992

The Location of Bound Lipid in the Lipovitellin Complex

P. A. Timmins,* B. Poliks, L. Banaszak

The location of the bound lipid in the soluble lipoprotein lipovitellin has been determined by neutron crystallographic techniques. With the use of the contrast variation method, whereby the crystals are soaked in different H_2O-D_2O mixtures, the lipid has been found to occupy a large cavity in the protein whose structure had previously been determined by x-ray crystallography. The lipid appears to be bound in the form of a bilayer with the major protein-lipid interactions being hydrophobic and with the lipid headgroups projecting into the bulk solvent and into a solvent-filled space in the cavity.

Existing molecular models of soluble lipoproteins are based mainly on physical methods that do not permit direct visualization of molecular structure. We describe neutron diffraction results which, when combined with an earlier x-ray crystallographic study, lead to a relatively complete three-dimensional model of a soluble lipoprotein called lipovitellin. The crystalline lipovitellin complex was derived from lamprey oocytes. It is comprised of three polypeptide chains, LV1, LV2, and PV, of molecular weight (M_r) 66,800, 40,750, and 35,200, respectively. PV, sometimes also called phosvitin, contains a significant number of phosphorylated Ser residues [for a relatively recent review, see (*1*)]. In addition to the protein components, the complex contains about 15% lipid, mainly in the form of phospholipids. The lipovitellin complex has been crystallized (*2*) and its structure solved to 2.8 Å resolution by x-ray crystallography (*3*) by using classical multiple isomorphous replacement (MIR) techniques. The resulting model, however, has some important limitations that may be summarized as follows. At the time when the model was constructed, the amino acid sequence was not known and the model was therefore described as a polyalanine chain. Although the complex is known to comprise ~1300 amino acids, the initial interpretation of the electron density based on multiple isomorphous replacement (MIR)

P. A. Timmins, Institut Laue-Langevin, 156X, 38042 Grenoble, Cedex 9, France.
B. Poliks, Department of Biological Chemistry, Washington University Medical School, St. Louis, MO 63110.
L. Banaszak, Department of Biochemistry, University of Minnesota Medical School, Minneapolis, MN 55455.
*To whom correspondence should be addressed.